Supporting Information for

"Electromagnetic interference shielding in 1-18 GHz frequency and electrical properties correlations in poly(vinylidene fluoride)-multi-walled carbon nanotube composites"

*G. Sudheer Kumar[1], Vishnupriya D.[1], Anupama Joshi[2], Suwarna Datar[2] and T. Umasankar Patro[1]**

[1]Departmentof Materials Engineering, Defence Institute of Advanced Technology, Girinagar, Pune 411025, India.

[2]Department of Applied Physics, Defence Institute of Advanced Technology, Girinagar, Pune 411025, India.

Functionalization of MWNT

Raman spectroscopy (HR 800, Horiba Jobin Yvon, Raman Spectrometer, France) of uf-MWNT and f-MWNT was recorded on powder samples using a He-Ne excitation laser source of λ ~632nm. Functionalization of MWNTs was investigated using Fourier transform infrared spectrometer (FTIR, 24V, 2A, (Alpha)-T, Bruker) in the range of 4000 to 1000cm^{-1}. Transmission electron microscopy (TEM) was carried out on a high resolution microscope (Tecnai G2, FEI, USA). The CNTs were dispersed in ethanol by ultrasonication and drop-cast on carbon coated copper grids. Thermogravimetric analysis (TGA) of CNTs was carried out using Simultaneous Thermal Analyzer (STA 6000 from PerkinElmer, USA). CNTs were heated from 30°C to 800°C at 20°C/min under nitrogen atmosphere with a flow rate of 80 mL/min.

Figure S1a presents the FTIR spectra of pristine (uf-MWNT) and acid functionalized MWNT (f-MWNT). The peak at 1290 cm^{-1} in FTIR of uf-MWNT (Fig S1a) is most likely due to the catalyst or impurities present in untreated CNTs. While the peaks at 1538 and 1295cm^{-1} for f-MWNT correspond to C=O and C-O stretching, respectively. The peaks at 2917 and 2847cm^{-1}

correspond to the -CH stretching and a broad peak at 3433cm^{-1} corresponds -OH stretching[1]. The peak at 1638cm^{-1} in pristine MWCNT corresponds to C=C stretching of CNT. These results indicate acid functionalization of CNTs, which are further corroborated by Raman spectroscopy. Figure S1b presents the Raman spectra for pristine MWNT and f-MWNT. As seen in the spectra, there are two prominent peaks at 1322 and 1593cm^{-1}, which correspond to D and G bands of CNT respectively. The G-band arises due to the tangential shear mode of carbon atoms due to the stretching in graphitic plane and the D-band due to defects present in the graphitic structure of CNTs[2]. The broad 2D peak at 2651cm^{-1} corresponds to second-order Raman scattering process[3]. The defects present in the CNTs were analyzed by taking the peak intensity ratios (I_D/I_G) for both uf-MWNT and f-MWNT. The I_D/I_G values for uf-MWNT and f-MWNT were found to be 0.81 and 0.84, respectively. From the intensity ratios, it can be inferred that the acid treatment has created more defects, though marginally, in the graphitic sheets of CNTs. The ratios of area under the D-band to G-band (A_D/A_G) peaks were computed and the values of which are found to be ~1.2 and ~2.0 for uf-MWNT and f-MWNT, respectively. These results indicate the formation of more defect sites on CNT surface due to acid functionalization.

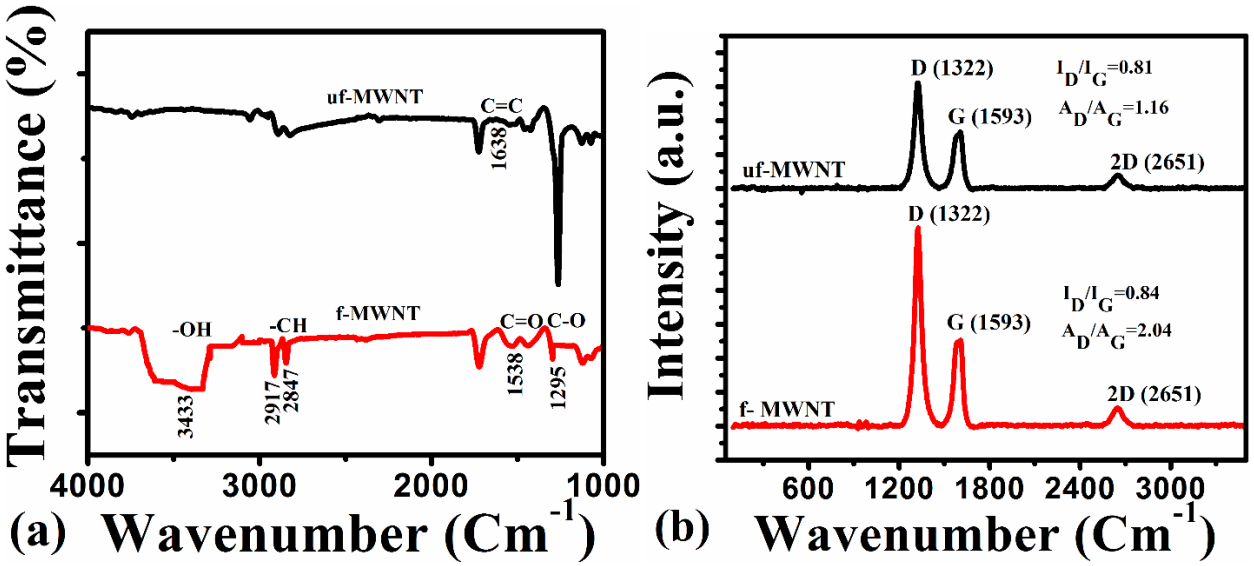

Figure S1. (a) FTIR spectra of the uf-MWNT and f-MWNT (b) Raman spectra of the uf-MWNT and f-MWCNT.

Figure S2 presents the TEM images of pristine (uf-MWNT) and acid functionalized MWNT (f-MWNT). The length of the CNT was not affected by the acid-treatment as it can be seen from Figure S2a-b. Figure S2a also shows the catalysts embedded in uf-MWNTs, which were removed by acid-treatment as seen in Figure S2b. This is corroborated by the decrease in diameter of CNTs upon acid-treatment.

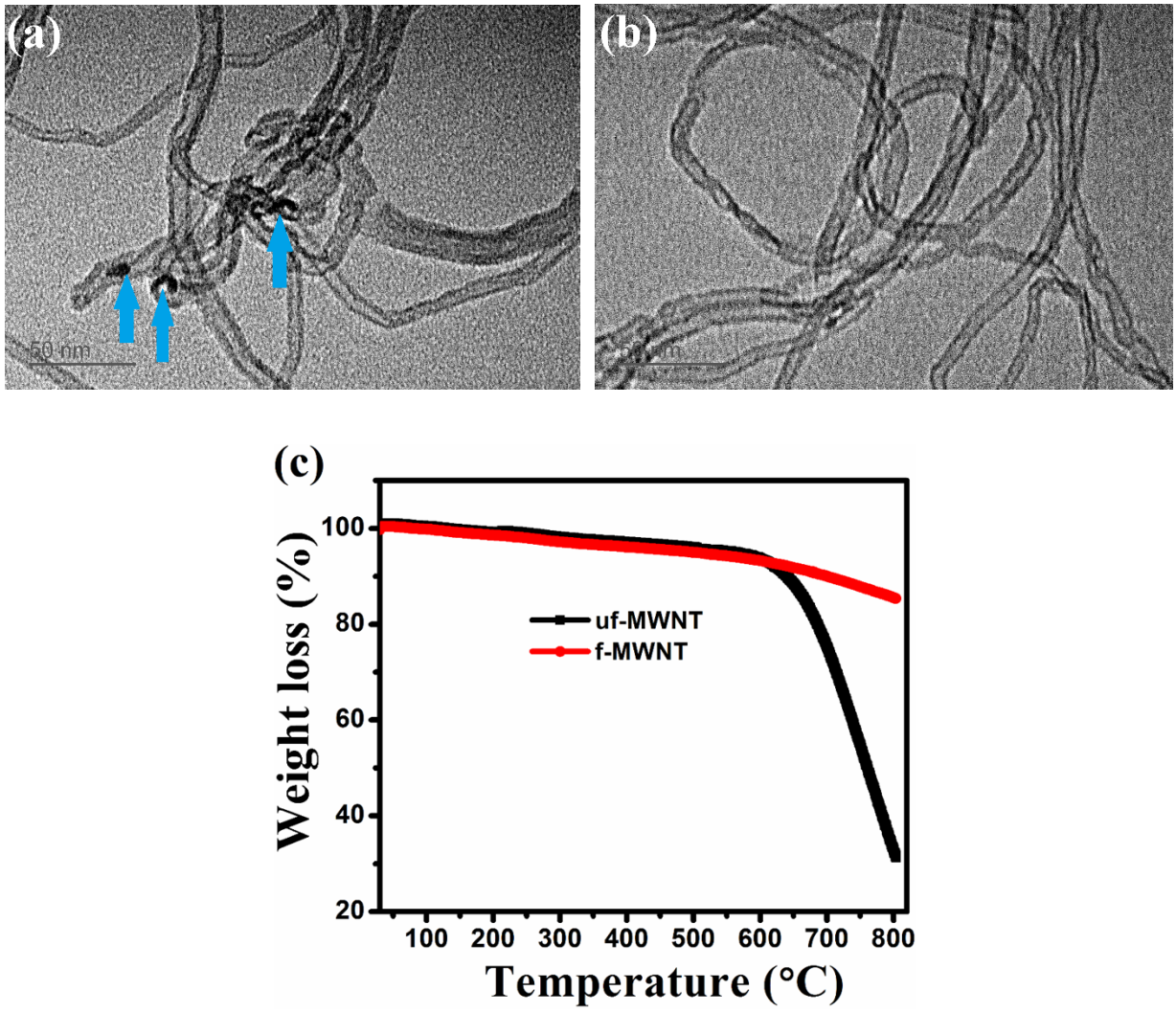

Figure S2. TEM images of (a) pristine (uf-MWNT) and (b) acid-functionalized CNTs (f-MWNT); (c) TGA curves of pristine MWNTs and acid functionalized MWNTs. The arrows in Fig. S2a show the presence of catalysts in as-received CNTs.

Impedance studies of MWNTs pellets

About 100mg of CNT powder was made into pallets in a stainless steel die of 20mm diameter using a hydraulic press (Atlas, 25Ton, UK). A load of 5 tons was applied for 5min. The thickness of the pallets was ~1 mm. The pallets were used for impedance measurements as obtained without applying conducting coating. The AC conductivities of uf-MWNTs and f-MWNTs pellets made from powder form in the frequency between 10^{-1} and 10^{7} Hz were measured by Impendence analyzer (Novocontrol, Germany).

Figure S3 presents the AC conductivity vs. frequency at room temperature for uf-MWNTs and f-MWNTs pellets. As expected, the conductivity of uf-MWNTs and f-MWNTs pellets in powder form are independent of frequency throughout the range. The conductivity values are not affected upon acid functionalization of CNT and are found to be in the order of ~10^{-3} S/cm for both pristine and acid functionalized CNTs pellets. This apparently indicates that there was a weak oxidation of CNTs, which did not affect the conductivity of CNTs.

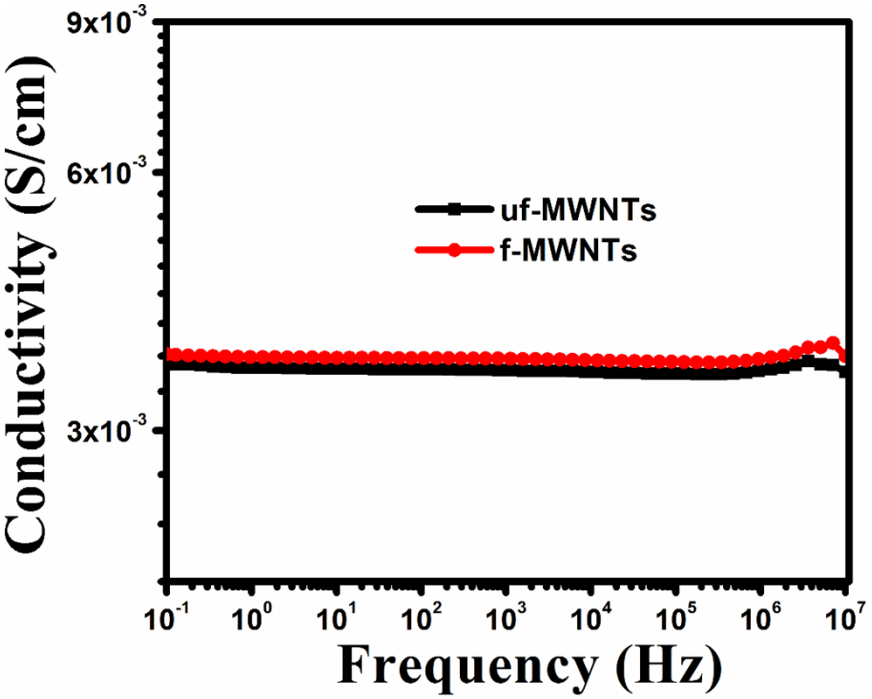

Figure S3. AC conductivity with frequency for uf-MWNT and f-MWNT.

Torque measurements during melt-mixing

The typical curves of the torque and temperature as a function of mixing time are presented in Figure S4a-c. The curves illustrate the thermo-mechanical properties of polymer and composites during mixing. As shown in Figure, initially the torque increased steeply with mixing time up to about 1min in case of PVDF (Fig. S4a) and ~30s in composites (Fig S4b-c) and then decreased and became steady for the rest of the mixing time, which indicates a uniform mixing. The initial increase of torque is due to the resistance of solid powder to the free rotation of the screws. In contrast, the temperature of the feed decreased initially and then increased and remained almost constant thereafter (Figure S4). The decrease in temperature in the initial stage is likely due to heat transfer from the chamber to the polymer. Figure S5 presents the average and maximum torque values for various composites. The maximum torque increased for the composites due to increase in CNT content indicating an increase in viscosity. Further it can be seen that the maximum torque was higher for uf-MWNT composites than that for f-MWNT for equal CNT weight fractions, which is likely due to higher resistance offered by pristine MWNTs while mixing as compared to functionalized CNTs.

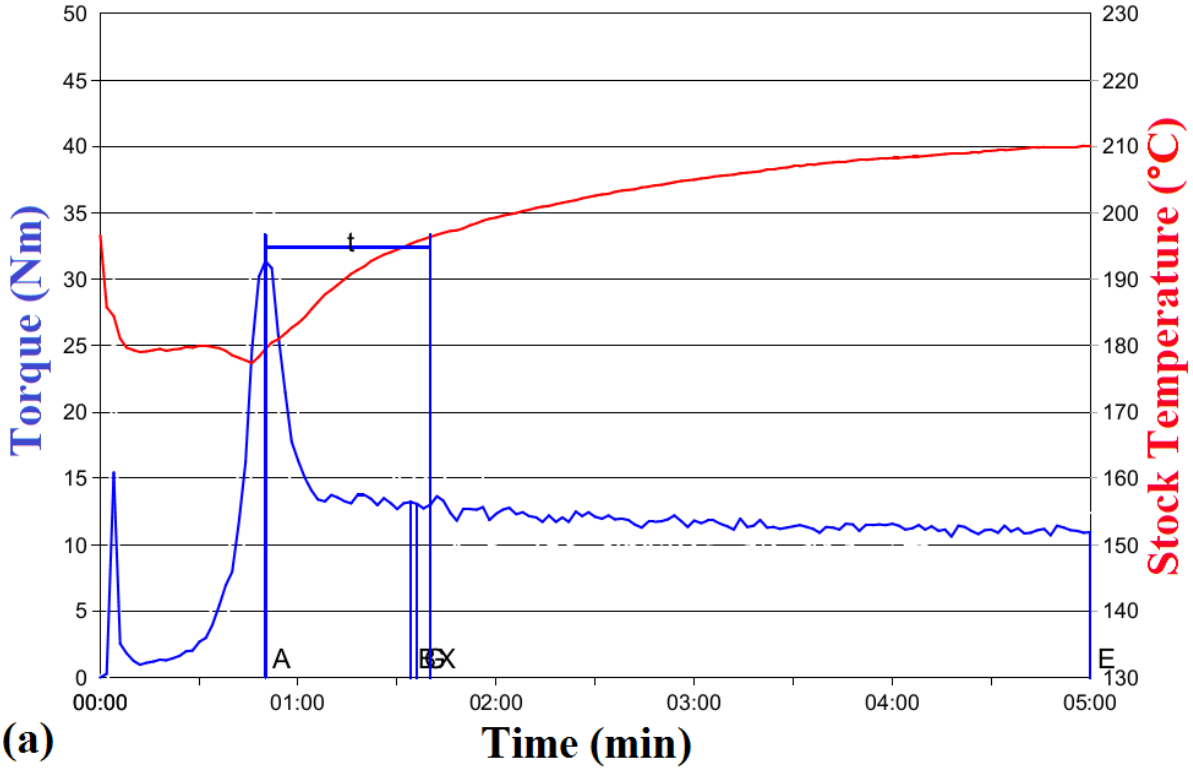
Torque (Nm)
Stock Temperature (°C)
Time (min)
t
A
E
00:00
01:00
02:00
03:00
04:00
05:00

(a)

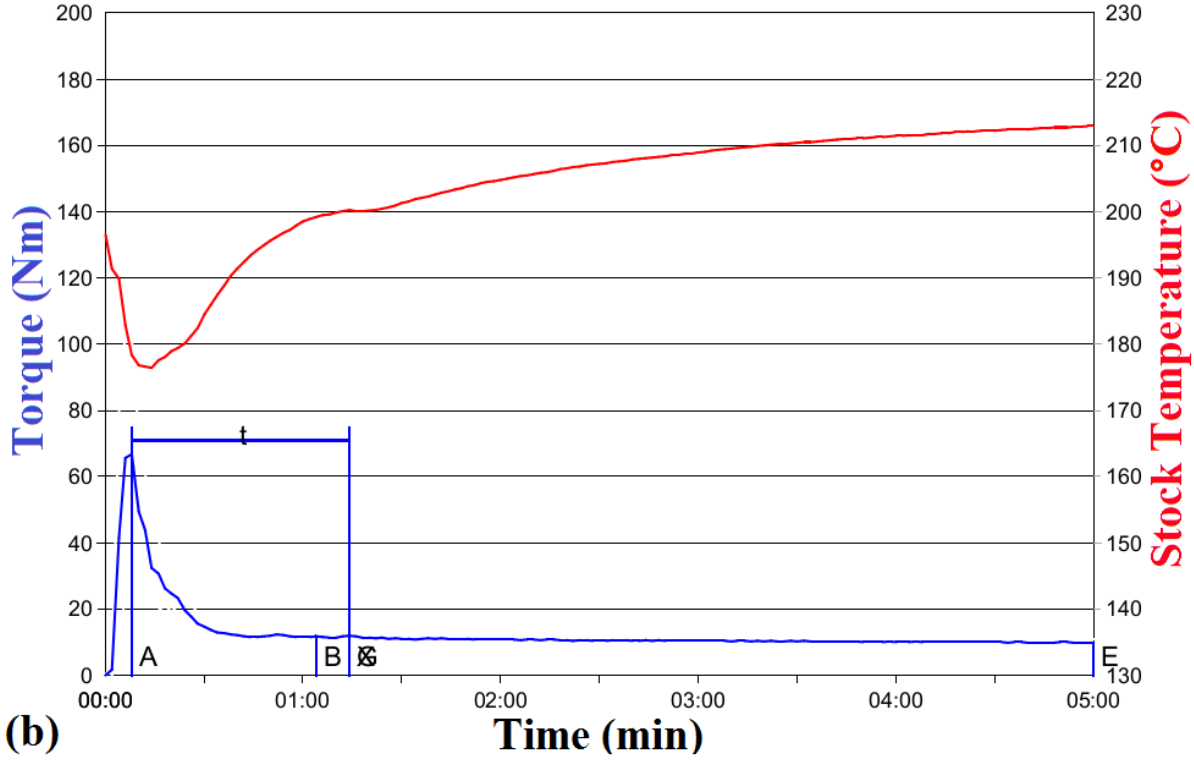
Torque (Nm)
Stock Temperature (°C)
Time (min)
t
A
E
00:00
01:00
02:00
03:00
04:00
05:00

(b)

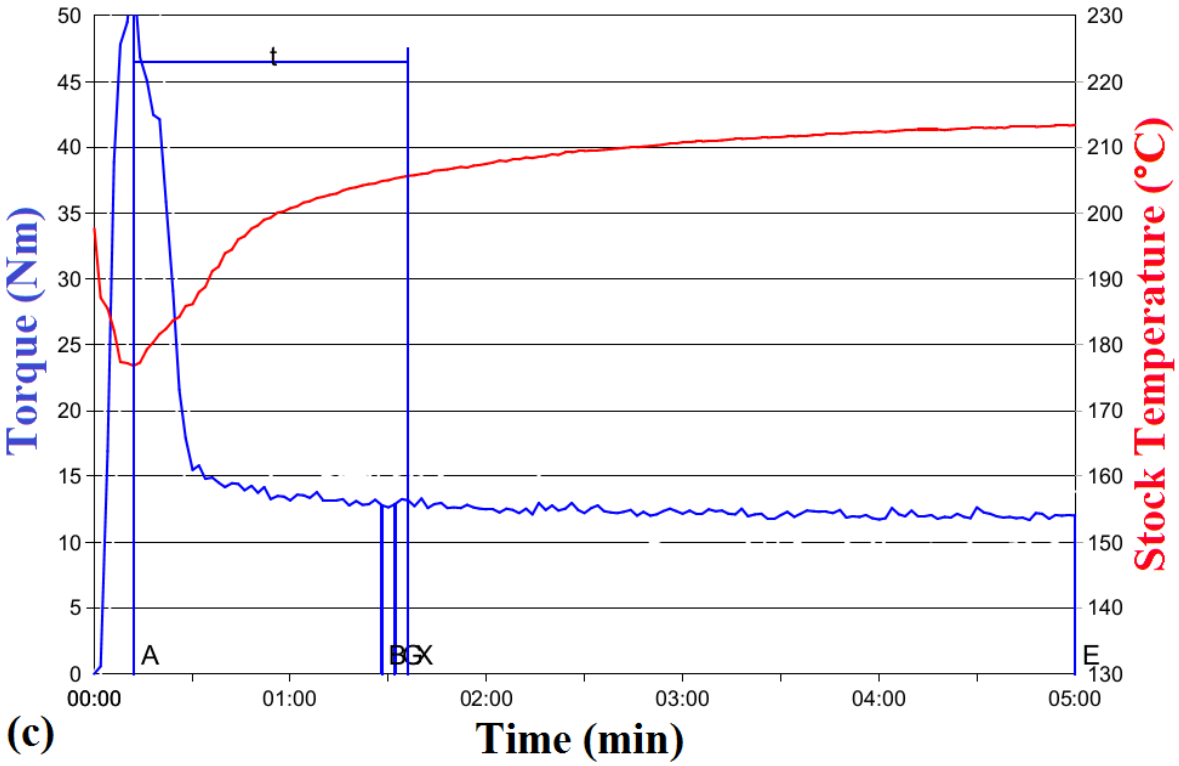

Figure S4. Torque vs. mixing time for (a) PVDF, (b) 4uf-MWNT and (c) 0.5f-MWNT composites.

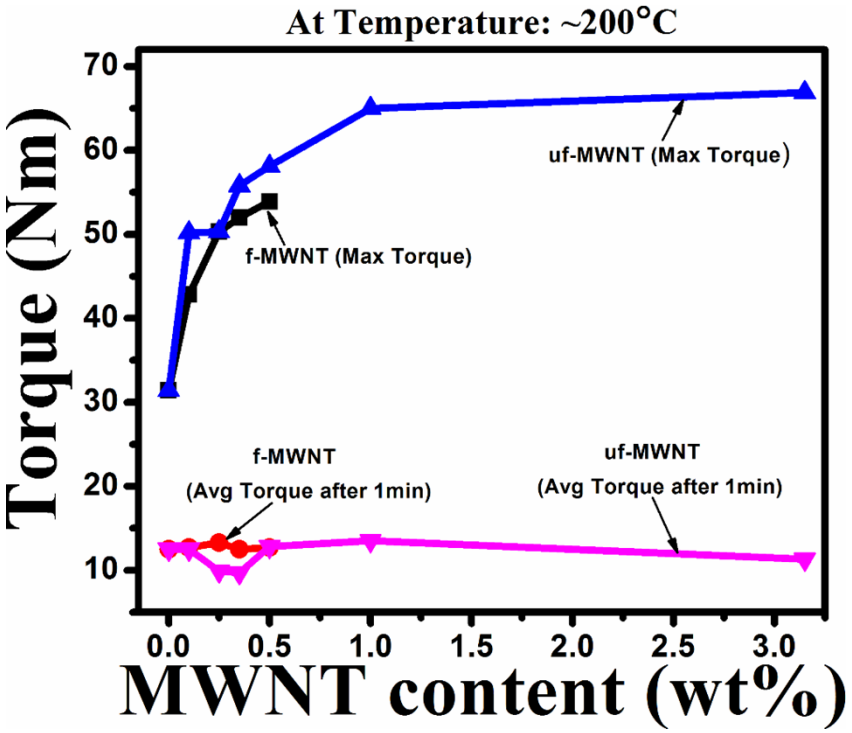

Figure S5. The average and maximum torque with MWNT content for composites, as obtained during melt-mixing.

Optical Images

The optical microscopy image of the composite films was taken at 10X using a Trinocular microscope Adicon Model ASD-600, India.

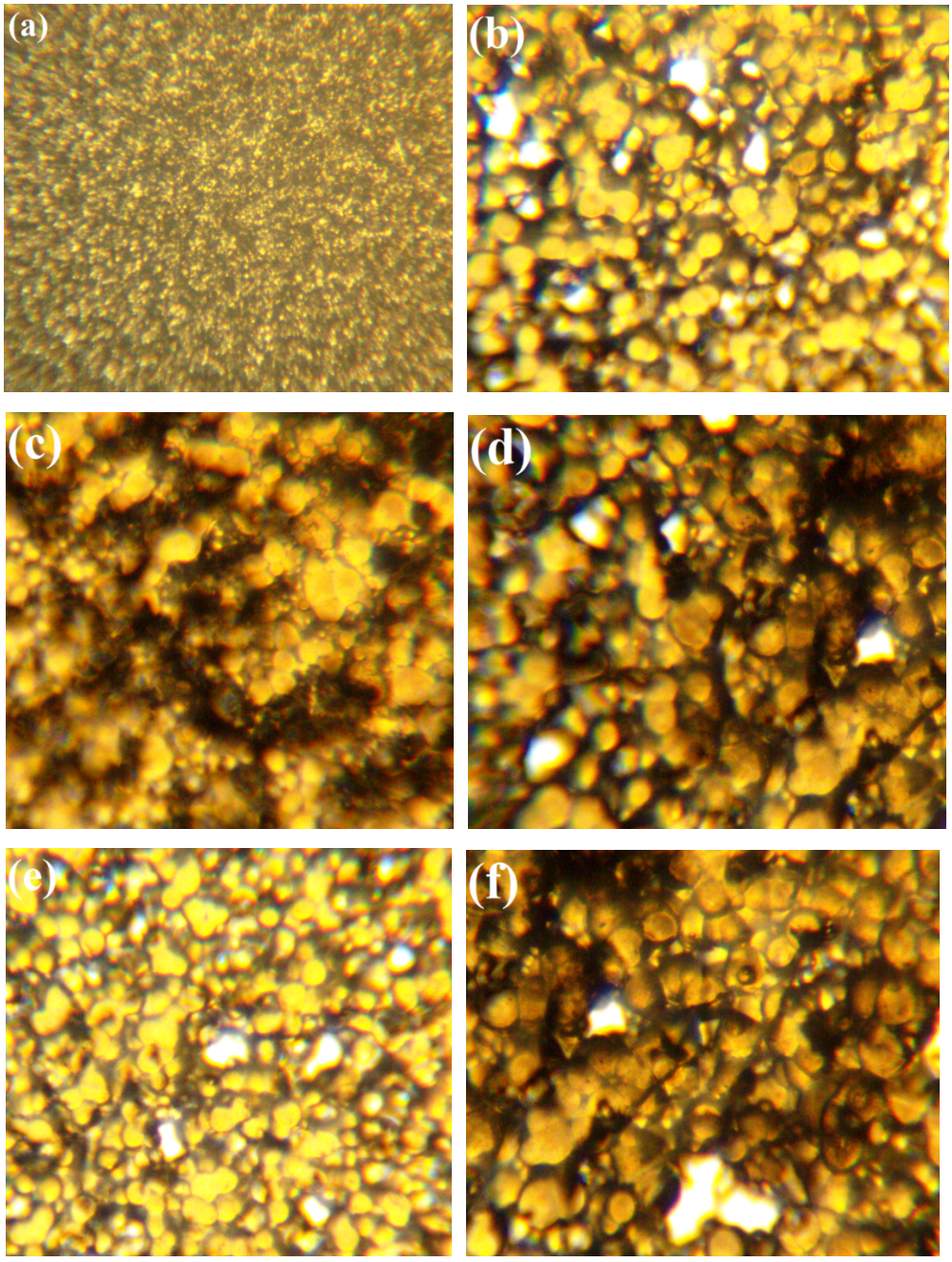

Figure S6. Optical images at 10X of (a) pure PVDF, (b) 0.1wt% uf-MWNTs in PVDF, (c) 0.35wt% uf-MWNTs in PVDF, (d) 0.5wt% uf-MWNTs in PVDF, (e) 0.1wt% f-MWNTs in PVDF and (f) 0.15wt% f-MWNTs in PVDF.

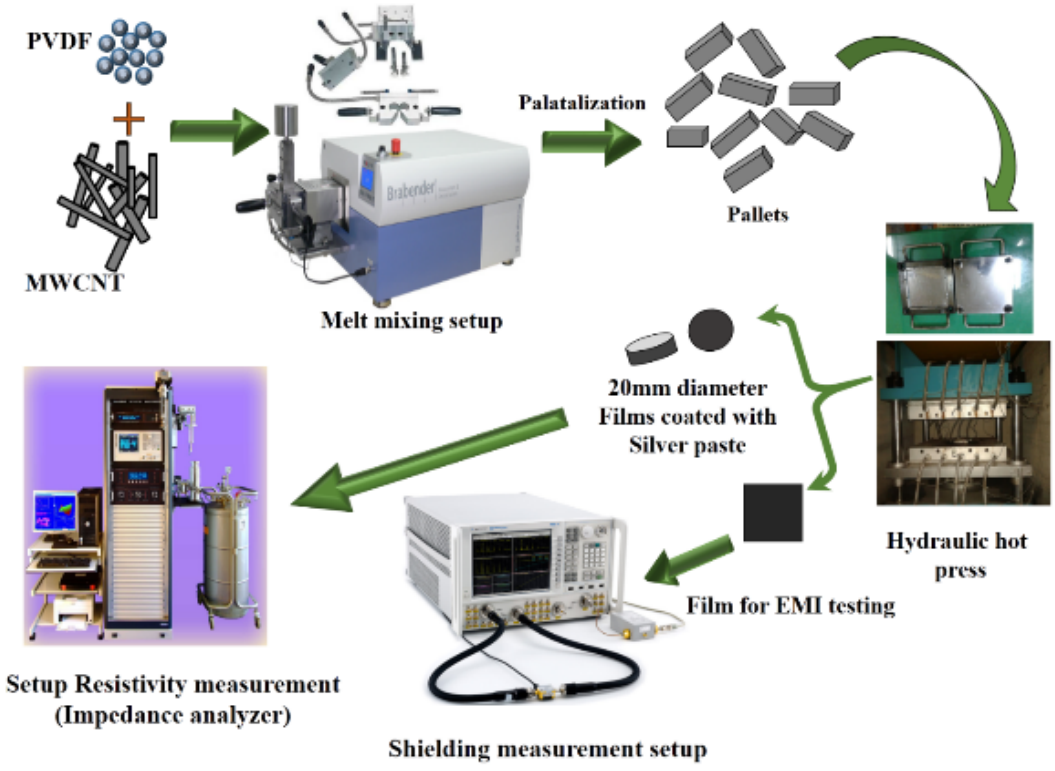

Figure S7. Schematic of PVDF composite fabrication and characterization.

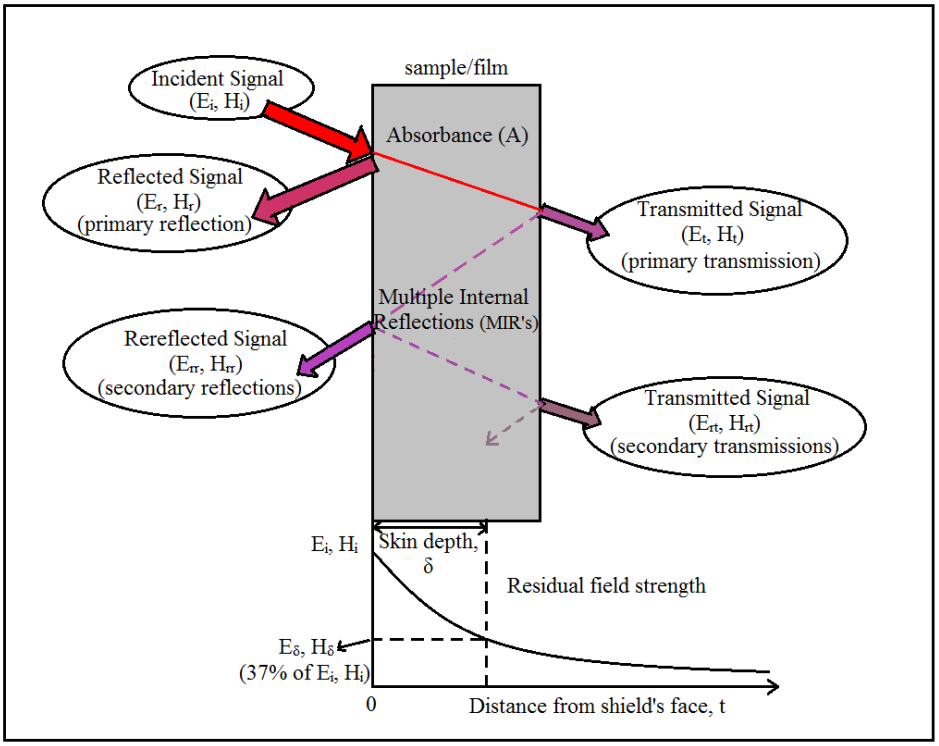

Figure S8. Graphical representation of EMI shielding mechanisms[4]

Figure of merit (FOM)

FOM of EMI SE is computed by using the following equation [5]. $FOM = \left(\frac{SE_{Comp} - SE_{PVDF}}{SE_{PVDF}} \right) \Big/ w$ Where SE_{Comp} and SE_{PVDF} are the total EMI shielding effectiveness of composite and pure polymer, respectively. The FOM of EMI SE for 0.5f-MWNT and 4uf-MWNT composites are presented in Table S1. It can be seen that the FOM increased significantly with CNT content. The reflectance and transmittance coefficients for the above composites at different frequencies are also presented in SI (Table S1).

Table S1. Figure of merit (FOM), Reflectance (R) and Transmittance (T) coefficients of 0.5fMWNTs and 4ufMWNTs composites at different frequencies

Bands and frequencies (GHz)		0.5f-MWNT composite			4uf-MWNT composite		
		FOM	R	T	FOM	R	T
L-Band	1.2	15	0.84	8.2×10^{-9}	20	0.86	5.6×10^{-10}
	1.5	281	0.68	3.8×10^{-6}	349	0.74	2.8×10^{-7}
	1.8	378	0.41	0.0003	505	0.57	3.5×10^{-5}
S-Band	2.5	157	0.32	0.013	165	0.32	0.012
	3	215	0.56	0.016	219	0.56	0.016
	3.5	156	0.32	0.034	156	0.33	0.034
C-Band	4.5	127	0.79	0.007	148	0.84	0.003
	5	35	0.77	0.009	44	0.75	0.004
	5.5	38	0.08	0.064	58	0.028	0.028
J-Band	6.5	159	0.18	0.054	234	0.29	0.017
	7	247	0.75	0.013	312	0.80	0.005
	7.5	204	0.64	0.018	257	0.70	0.007
X-Band	9	5413	0.74	5.3×10^{-5}	6450	0.77	7.2×10^{-6}
	10	5050	0.61	5.6×10^{-5}	6400	0.59	5.5×10^{-6}
	11	336	0.77	4.4×10^{-5}	431	0.81	3.3×10^{-6}
Ku-Band	15	26	0.36	0.296	--	--	--
	17	8	0.51	0.043	--	--	--

References:

(1) B. P. Singh, D. Singh, R. B. Mathur and T. L. Dhami, *Nanoscale Res. Lett.*, 2008, **3**, 444-453.

(2) S. K. Rath, S. Dubey, G. S. Kumar, S. Kumar, A. K. Patra, J. Bahadur, A. K. Singh, G. Harikrishnan and T. U. Patro, *J. Mater. Sci.*, 2014, **49**, 103-113.

(3) V. Eswaraiah, V. Sankaranarayanan and S. Ramaprabhu, *Nanoscale Res. Lett.*, 2011, **6**, 137.

(4) P. Saini, V. Choudhary, B. P. Singh, R. B. Mathur and S. K. Dhawan, *Synt. Met.*, 2011, **161**, 1522-1526.

(5) J. Yuan, S. Yao, W. Li, A. Sylvestre, and J. Bai, *J. Phys. Chem. C*, 2014, **118**, 22975-22983